LAAS Position Domain Monitor Analysis and Test Results for CAT II/III Operations

Jiyun Lee

Stanford University

BIOGRAPHY

Jiyun Lee received a B.S degree from Yonsei University, Seoul, Korea (1997), the M.S. from the University of Colorado at Boulder (1999), in Aerospace engineering and Science, and the M.S from Stanford University, Stanford, CA (2001), in Aeronautics and Astronautics. She is currently a Ph.D. candidate at Stanford University, working on GPS Local Area Augmentation System.

ABSTRACT

The Local Area Augmentation System (LAAS) is a differential GPS navigation system being developed to support aircraft precision approach and landing with guaranteed accuracy, integrity, continuity and availability. While the system promises to support Category I operations, significant technical challenges are encountered in supporting Category II and III operations. The primary concern has been the need to guarantee contentment with stringent requirements for navigation availability. This paper describes how Position Domain Monitoring (PDM) may be used to improve system availability by reducing the inflation factor for standard deviations of pseudorange correction errors. The role of PDM in mitigating the continuity and integrity risks are also presented with recent test results.

1.0 INTRODUCTION

LAAS navigation integrity is quantitatively appraised by the position bounds that can be ensured with an acceptable level of integrity risk. In this regard, aircraft compute the vertical protection level (*VPL*) and the lateral protection level (*LPL*) as position error limits assuming a zero-mean, normally distributed fault-free error model for the broadcast pseudorange corrections. User integrity thus relies on the standard deviations of pseudorange correction errors that are broadcast by the LAAS Ground Facility (LGF) along with the corrections, as these "sigmas" are used in the calculation of *VPL* and *LPL*. The bounding standard deviation of correction error, or σ_{pr_gnd}, is broadcast for each satellite approved by LGF integrity monitoring [1-3].

One significant integrity risk is that the standard deviation of pseudorange correction error grows to exceed the broadcast correction error sigma during LAAS operation. A great deal of prior work has been done to insure that the zero-mean Gaussian distribution implied by the broadcast sigma values "overbounds" the tails of the true distribution (possibly non-Gaussian and non-zero-mean)[4]. This is done by broadcasting an inflated σ_{pr_gnd} and detecting violations of this overbound (due to unexpected anomalies) using sigma monitors.

Given that an enhanced LGF architecture is required to meet Category II/III requirements, the Position Domain Monitor (PDM) concept has been proposed in [5]. In this concept, the Position Domain "Remote" Receiver hosting the PDM derives position solutions from the current LGF corrections using all visible satellites approved by the LGF and all reasonable subsets of these satellites that an aircraft may be limited to using. These position solutions are compared to the known (surveyed) location of the PDM antenna, and errors exceeding the detection threshold would be alerted. The current LGF does not use PDM – it monitors each GPS measurement individually and approve individual satellites in range domain. In previous work, Stanford University has developed PDM algorithms and demonstrated that this approach could improve upon the existing sigma monitoring [6].

The LAAS sigma overbounding issue remains difficult to solve. One reason is that high levels of sigma inflation cannot be tolerated for Category II/III approaches because of the tightened Vertical Alert Limit (VAL – a bound on maximum tolerable VPL) and high availability requirements (0.999 or higher, depending on the airport). In this paper, Section 3 discusses the characteristics of error distributions in the position domain and demonstrates that the PDM supports smaller σ_{pr_gnd} inflation factors needed for Category II/III operations. The unique, detailed approach to estimate σ_{pr_gnd} inflation factors is presented in Section 4. Improved pseudo-user's

performance, as demonstrated with the hardware configuration in Section 2, is discussed in Section 5. Overall the PDM, as an addition to the LGF architecture, makes it possible to meet the availability requirement of Category II/III operations.

Furthermore, the addition of the PDM helps improve the continuity and integrity of Category II/III operations. Section 6 examines a proposed methodology to enhance the average continuity with the PDM outputs. The focus of Section 7 is the application of Cumulative Sum (CUSUM) method to the PDM. The results of the PDM-CUSUM nominal and failure tests demonstrate that PDM can provide extra integrity in the event of unexpected sigma violations.

2.0 STANFORD LGF PROTOTYPE ARCHITECTURE

Stanford University researchers have developed an LGF prototype known as the Integrity Monitor Testbed (IMT). The purpose of the IMT is to evaluate whether an operational LGF can meet its requirements for navigation integrity and continuity for Category I precision approach. While the Category I IMT is essentially finished, it would be desirable to satisfy Category II/III requirements with modifications to the existing LAAS architecture. To support this, a prototype of the PDM was added to the Stanford IMT. In order to test a capability of meeting Category II/III precision approach requirements with high availability, a LAAS "pseudo-user" receiver was set up within the IMT-PDM installation.

Figure 1: Stanford LGF Hardware Configuration Performance Test-bed

Figure 1 shows the configuration of the original three IMT antennas on the Stanford HEPL laboratory rooftop as well as the PDM antenna on the Stanford Durand building and the "pseudo-user" antenna on top of a nearby parking structure. The existing IMT antennas are connected to three NovAtel OEM-4 reference receivers, which are connected to the IMT computer by a multiport serial board. The LGF requires redundant DGPS reference receivers to be able to detect and exclude failures of individual receivers. The separations between these three NovAtel Pinwheel (survey grade) antennas are limited to 20 – 65 meters by the size of the HEPL rooftop but are sufficiently separated to minimize correlation between individual reference receiver multipath errors (this has been demonstrated in previous work) [7]. The PDM uses the existing Stanford WAAS Reference Station antenna, which is separated by approximately 150 meters from the IMT antennas. The pseudo-user's NovAtel Pinwheel antenna is apart from the IMT by approximately 230 meters and from the PDM by approximately 360 meters. The NovAtel OEM-4 receivers connected to the PDM and "pseudo-user" antennas collect pseudorange measurements, carrier-phase measurements, and navigation messages from GPS satellites.

The PDM and "pseudo-user" receivers are set up to collect measurements at the same time as the remainder of the IMT. These measurements are post-processed in a single computer where the algorithms are developed and tested. Position solutions of both the PDM and "pseudo-user" are computed in the manner required of the LAAS airborne receivers (as specified in the RTCA LAAS *Minimum Operational Performance Standards*, or MOPS [1]) to mirror LAAS aircraft operations to the degree possible. In order to estimate the user's performance improvement that results from adding the PDM, one post-processing run is conducted with existing IMT measurements only, and a second run is conducted with the combined IMT-PDM algorithms.

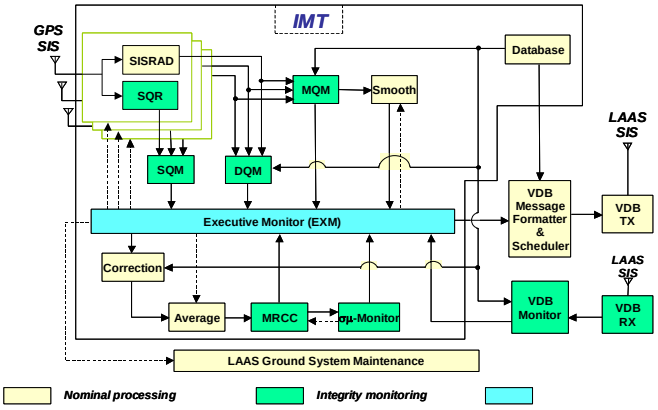

Figure 2: IMT Functional Block Diagram

Figure 2 shows the IMT functional block diagram. The Signal-in-Space Receive and Decode (SISRAD) function provides pseudorange measurements, carrier-phase measurements, and navigation data messages that are the core of IMT processing and enables the generation of carrier-smoothed code differential corrections. The resulting LAAS corrections, which are used to derive user position solutions, are also applied to the processing of the PDM and evaluation of user's performance.

The LGF is not only responsible for generating and broadcasting corrections but also for detecting and alerting a wide range of possible failures in the GPS Signal in Space (SIS) or in the LGF itself. In this regard, IMT processing utilizes several different types of monitoring algorithms [8]. In order to isolate and remove error sources (some of which may trigger more than one monitoring algorithm), Executive Monitoring (EXM) is included in the IMT as a complex failure-handing logic. The PDM also supports enhanced EXM in the LGF by better separating faults that must be excluded from those that can be tolerated.

3.0 POSITION DOMAIN MONITOR

3.1 POSITION DOMAIN MONITOR ALGORITHMS

PDM applies the carrier-smoothing filter with the same method performed in the IMT, to reduce raw pseudorange measurement errors [2, 9, 10]. The set of LGF differential corrections are applied to the current carrier-smoothed code measurements to form position solutions based upon the requirements of the LAAS MOPS [1]. The PDM computes positions using a linearized, weighted least squares estimation method as shown in Appendix A. These position solutions are compared to the known location of the PDM antenna.

3.2 ERROR DISTRIBUTIONS IN POSITION DOMAIN

Clearly, the inflation factor of the sigma that bounds range or position-domain errors is a strong function of the actual error distributions. In this regard, the analysis on error distributions was performed before deriving inflation factors. This analysis investigates the conversion of range domain error statistics to position domain error statistics. The relationship between pseudorange correction errors and user position errors is

$$\Delta x = s_1(\Delta y_1 - b_1) + s_2(\Delta y_2 - b_2)... + s_n(\Delta y_n - b_n) \quad (1)$$

where Δy_i is the pseudorange correction error, and b_i is the mean bias of correction errors, for each satellite i. The position error, Δx, is the sum of mean-biased correction errors, which are also weighted by coefficients of the projection matrix, s_i (see Appendix A).

The probability density function (PDF) of the sum of the weighted and mean-biased independent variables is convolution of their respective scaled and mean-shifted PDF's, as shown by the application of the Central Limit Theorem. Based on equation (1) and the Central Limit Theorem, the probability density function of position errors is

$$f(\Delta x) = \frac{1}{s_1} f(\frac{\Delta y_1 - b_1}{s_1}) * \frac{1}{s_2} f(\frac{\Delta y_2 - b_2}{s_2}) * ... \frac{1}{s_n} f(\frac{\Delta y_n - b_n}{s_n}) \quad (2)$$

where the terms $f(\Delta y_i)$ represent the probability density function of pseudorange correction errors, for each satellite i.

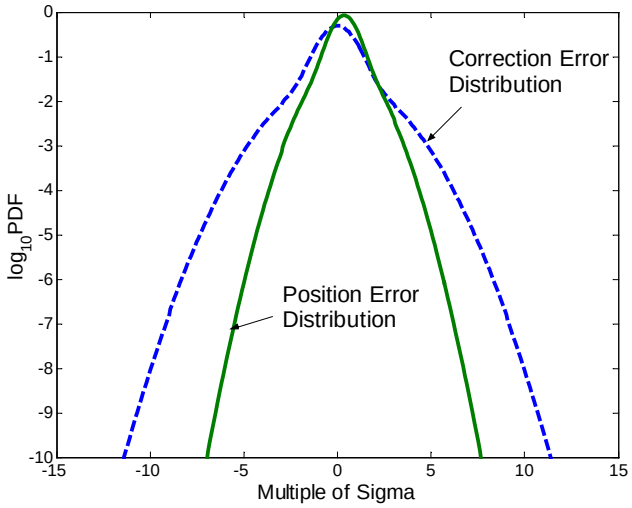

Figure 3: Error Distributions in Position Domain and in Range Domain

A theoretical model of correction error distributions (dashed curve in Fig.3) has been developed as described in Section 4.2 in this paper. By convolving the correction error PDF's, which are differently scaled and mean-shifted, the position error distribution is found as shown in Figure 3. The weighting parameters, S_i, and mean-bias parameter, b_i, are carefully selected in this analysis, so that the established error model in position domain is a good representation of the empirical data. Under the condition that parameters have nominal values, the tails of the position error distribution are thinner than those of the individual correction error distributions.

4.0 SIGMA INFLATION FACTOR ESTIMATION

LAAS navigation integrity is realized through the computation of protection levels at the user aircraft. A basic assumption of computing protection levels is that the differentially corrected pseudorange errors are zero-mean Gaussian distributed. In practice, the error distribution may not be exactly Gaussian, due to the time-varying environmental conditions, such as ground reflection multipath. The pre-estimated sigma is also subject to the uncertainty, since the finite number of samples is available in general. In order to account for these, sigma inflation is needed to provide safety margin on protection bounds [2, 3, 11]. Each error sources are considered separately in this analysis. Each estimated inflation factors for mitigating integrity risks are then combined to one inflation factor of the broadcast sigma

4.1 INFLATION FACTOR TO COVER FINITE SAMPLE SIZES

The broadcast value of sigma must account for specific environmental conditions (such as antenna sitting, gain pattern, and system configuration) of each LGF sites.

Even though the environment is assumed to be stationary, the pre-estimated sigma may have a statistical noise due to the limited number of sample sizes. As regarding, the previous work has been done to investigate the sensitivity of integrity risk to statistical uncertainties, to which the correction error standard deviation and error correlation between multiple reference receivers are susceptible [11, 12]. Based on this work, the minimum acceptable buffer for the broadcast sigma was determined as 1.2.

4.2 INFLATION FACTOR TO COVER MIXING OF PROCESS

The error distribution may change with time, as the environment condition varies. In addition, the mixing of errors, such as ground reflection multipath, makes the error distribution difficult to be characterized. The correction errors shown in Fig.4 as a dotted curve clearly form a non-Gaussian distribution. The LGF B-values, collected at the Stanford IMT, are used to establish the actual pseudorange correction error distribution. Since the B-values represent pseudorange correction differences across reference receivers (ideally, the pseudorange corrections from all reference receivers should be the same for a given satellite), the B-values represent pseudorange correction errors that would exist if a given reference receiver has failed [2, 10, 13]. The limited number of sample sizes makes a theoretical model necessary for estimating the inflation factor. The Gaussian-Mixture distribution used as a theoretical model is

$$f_{GM} = (1-\varepsilon) * N(\mu_1, \sigma_1) + \varepsilon * N(\mu_2, \sigma_2) \quad (3)$$
$$; \quad \varepsilon = 0.15, \mu_1 = \mu_2 = 0, \sigma_1 = 0.75, \sigma_2 = 1.82$$

where $N(\mu,\sigma)$ is a normal distribution with mean, μ, and sigma, σ. This model (green solid curve) shown in Fig. 4 well characterizes the actual distribution of Gaussian-core and non-Gaussian tails. Note that the scale of the vertical axis is logarithmic. In order to cover the tails of non-Gaussian distribution, sigma should be inflated. To meet integrity requirement of 1.2×10^{-10} for Category II/III under the hypothesis of fault-free conditions (H0), the minimum tolerable inflation factor is 2.32. The Gaussian distribution with inflated sigma by 2.32 is shown as a red solid curve in Fig.4.

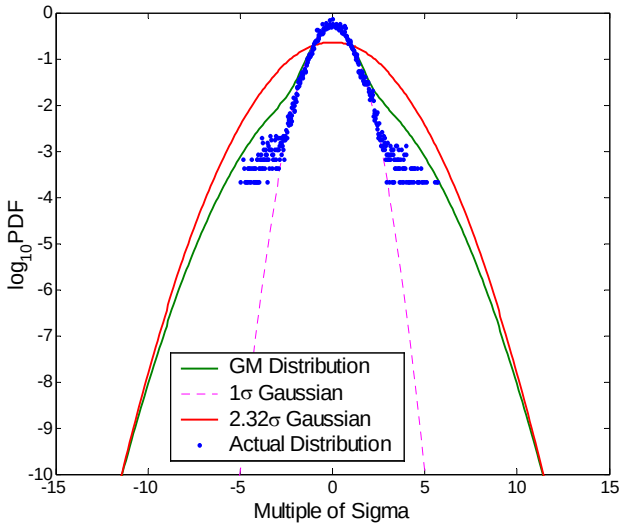

Figure 4: Probability Density Function of the Normalized B-values (Error Distribution in Range Domain)

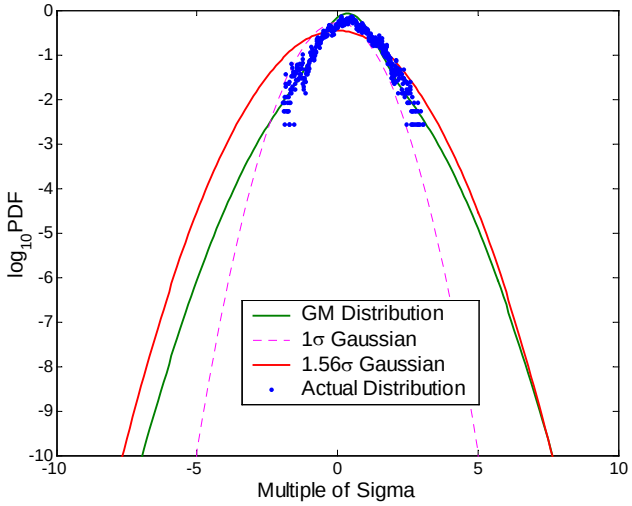

Figure 5: Probability Density Function of the Normalized Vertical Position Errors (Error Distribution in Position Domain)

As proven in Section 3.2 in this paper, the tail of error distributions becomes thinner when converted to the error distribution in position domain. The actual distribution (dotted curve) of normalized vertical position errors is plotted in Fig.5. A theoretical model is set again to determine the inflation factor, with which the tail probability of the order of 10^{-10} is bounded. The resulting buffering parameter is 1.56. Note that test statistics are highly dependent on the system configuration, and thus these analyses should be conducted for individual LGF sites.

4.3 INFLATION FACTOR TO COVER LIMITATION OF SIGMA MONITORS

The possibility of sigma violation exists not only because of nominal sigma uncertainty but also because of unexpected anomalies. As regards, sigma monitors are designed to provide the necessary integrity in the event that the true sigma exceeds the broadcast sigma [4]. If the integrity risk exceeds the total allocated risk, such sigma failure is defined as "minimal risk increase", and should be detected within a day based on time-to-alert requirements. However, the current sigma monitors have limitations on mean detection time[4], which should be covered with an additional inflation factor.

4.3.1 Gaussian Assumption on Error Models

By definitions, out-of-control sigma (σ_{ooc}) greater than the inflation factor, falls into "minimal risk increase" (i.e. the actual sigma exceeds the broadcast sigma) and should be alarmed within a day.

$$\sigma_{out-of-control} = \frac{\sigma_{Actual}}{\sigma_{Theoretical}} \tag{4}$$

$$Inflation \quad Factor = \frac{\sigma_{Broadcast}}{\sigma_{Theoretical}}$$

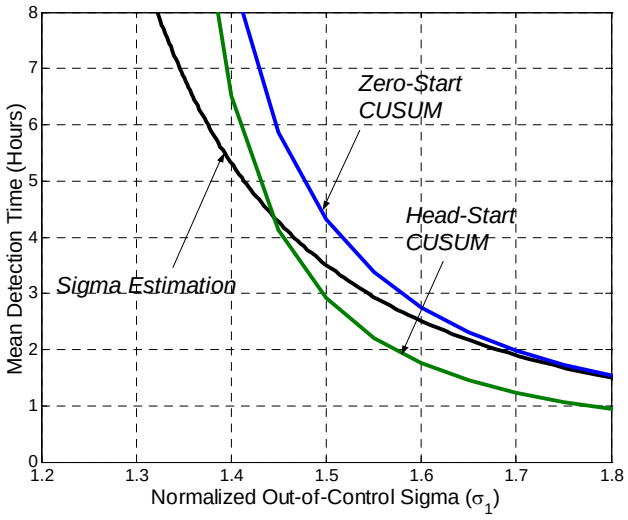

Figure 6: Failure-State *Average Run Lengths* for CUSUM and Sigma Estimation Monitors

Fig.6 shows average times for each sigma monitor to take to detect certain failure-states in the condition that error distributions are Gaussian. Assuming that the average time-length of continuous data in one satellite pass is 5 hours, the minimum σ_{ooc} detectable within a day is 1.41. Accordingly the inflation factor should be greater than 1.41.

4.3.2 Non-Gaussian Assumption on Error Models

As addressed in Section 4.2 in this paper, the error distribution may not be precisely Gaussian. As regards, the corresponding results to Fig.6 are generated using the Non-Gaussain model described in Equation (3). The resulting minimum σ_{ooc} detectable within 5 hours is 1.58. Thus, the inflation factor should be greater than 1.58.

4.4 TOTAL INFLATION FACTOR

The inflation factor for the broadcast sigma should be determined considering all conditions discussed in Section 4.1,4.2 and 4.3.

- Theoretical (or pre-estimated) sigma are to be inflated by a factor of 1.2 to cover the effect of finite sample sizes (Section 4.1)
- Inflation factors to cover the tail of non-Gaussian distributions are 2.32 in range domain and 1.56 in position domain respectively (Section 4.2)
- The total inflation factor should be at least 1.58 to overcome the limitation of existing sigma monitors (Section 4.3)

The total estimated inflation factors are shown in Table 1. Since the conditions described in Section 4.1 and 4.2 are independent, the resulting factors are multiplied. Both total inflation factors, induced based on error statistics in range domain and position domain, are greater than 1.58, which satisfies the third condition. Inflation factors derived here are used to compute vertical protection levels and to evaluate the system performance in the following section.

Table 1. Total Inflation Factors

Range Domain	1.2x2.32 = **2.78**
Position Domain	1.2x1.56 = **1.87**

5.0 PSEUDO-USER'S PERFORMANCE

An additional static receiver, placed to validate the performance of "pseudo-user", uses the LGF pseudorange corrections to form position solutions, which are compared to the surveyed location of the pseudo-user's antenna. The LAAS MOPS specify the computation of position solutions [1]. In order to represent the expected performance of Category II/III LAAS installations, the Accuracy Designator C (AD-C) is applied to the pseudorange error model [14]. The details of the procedure are described in Appendix A.

In the LAAS, the final quantitative appraisal of navigation performance is realized through the computation of protection levels. As regards, the user computes VPL for H0 hypothesis as follows:

$$VPL_{H0} = K_{ffmd} \sqrt{\sum_{i=1}^{N} S_{vert,i}^2 (f \cdot \sigma_i)^2} \tag{5}$$

where f is the inflation factor and K_{ffmd} is multiplier which determines the probability of fault-free missed detection [1]. K_{ffmd} is equal to 6.441 when the number of ground reference receivers is 3. $S_{vert,i}$ is coefficients of the vertical row of the projection matrix.

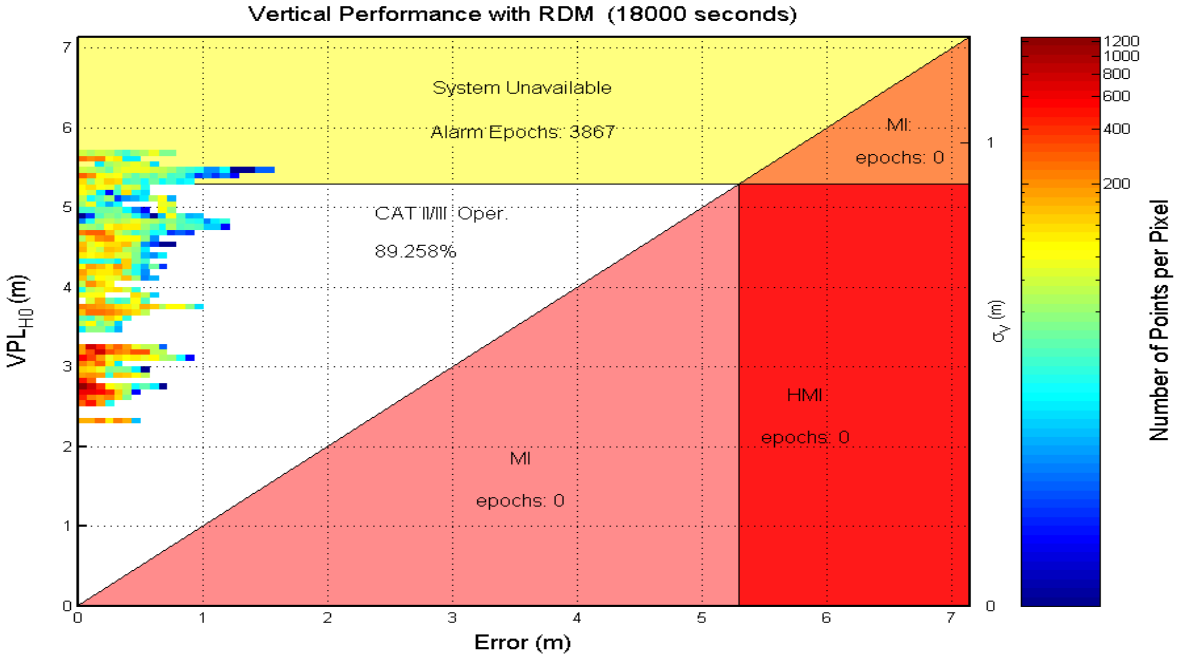

Figure 7: Pseudo-User's System Performance in Vertical Direction with Range Domain Monitor

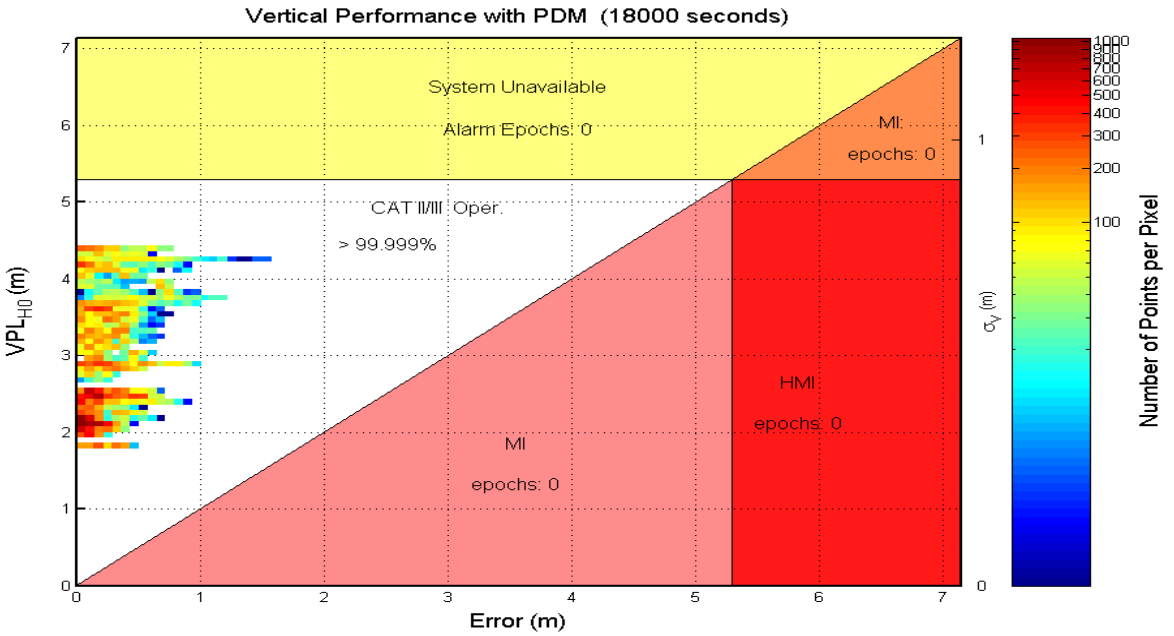

Figure 8: Pseudo-User's System Performance in Vertical Direction with Position Domain Monitor

The Figure 7 shows the vertical system performance achieved with the current range domain monitor only. The horizontal axis is the vertical position error (*VPE*) and the vertical axis is the vertical protection level. Note that the inflation factor, *f*, applied in Equation (5) is 2.78. Each bin represents the number of occurrences of a specific

(error, protection level) pair and the color of each grid indicates the total number of epochs that pair occurred (the copyright of the MATLAB code used to generate Fig.7 and 8 at the Stanford WAAS laboratory). The *VPE*s are always less than 2 meters, which is defined as an accuracy requirement of Category II/III approach. Integrity risk is defined as the probability that the position error exceeds the alert limits and the navigation system alert is silent beyond the time-to-alarm. The event with *VPL* less than the vertical alert limit (*VAL*) but error greater than the *VAL*, which leads to Hazardously Misleading Information (*HMI*), indicates a violation of integrity. In any case, the errors are always less than the *VPL* and also *VAL*. Any points are not considered as the integrity failure of the navigation system.

LAAS availability is defined as the fraction of time for which the system is providing position fixes to the specified level of accuracy, integrity and continuity. If the computed protection level exceeds the corresponding alert limit then the system is no longer operational and loses its availability. The *VAL* for Category II/III precision approach, indicated by the horizontal and vertical lines in Fig.7, is set in the LAAS System Specification at 5.3 meters. As shown in Fig.7, The system availability achieved in this analysis is only 89.258 %. Thus the system with range domain monitor only cannot meet the availability requirement of the Category II/III approach, which is a probability of 99.999%.

The position domain monitor supports the Category II/III operations by reducing the sigma inflation factor. The pseudo-user's vertical performance provided with the position domain monitor is shown in Fig. 8. Here, the sigma inflation factor of 1.87 is applied to compute VPLs. As a result, the system maintained greater than 99.999% availability in vertical positioning.

6.0 USE OF SCREENING PROCESS

The integrity checks with satellite (SV) outages are needed to cover cases where user aircraft is not tracking all SV's approved by LGF. As concerns, a screening process determines the satellite subsets to be processed by the PDM [6]. These subsets are the various possible combinations of satellites that a user receiver could process in its position solution. This includes the "all approved SV in view" case (approved by the LGF prior to the PDM taking action), all "one-SV-out" combinations, and all "two-SV-out" combinations.

The PDM outputs after the screening process could be used to improve LGF performance [15]. A key assumption of Category II/III LGF monitoring is that all airborne users have *VPL*s right at the 5.3-meter maximum imposed by the *VAL*. In practice, the truth is certainly better as shown Figure 8. If the worst computed *VPL* from the PDM outputs (*W_VPL*) is less than *VAL*, the effective VPL_{H0} can be made to be equal to *VAL* by increasing the integrity monitor detection thresholds. This leads the effective Minimum Detectable Errors (MDE) to be increased. After this process, the continuity risk is significantly lowered while maintaining the required integrity.

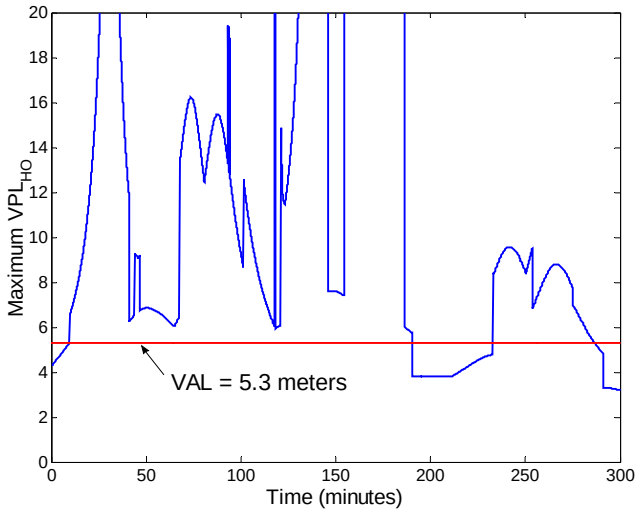

Figure 9: The Worst-case VPL_{HO} Out Of All "Two-SV-Out" combinations

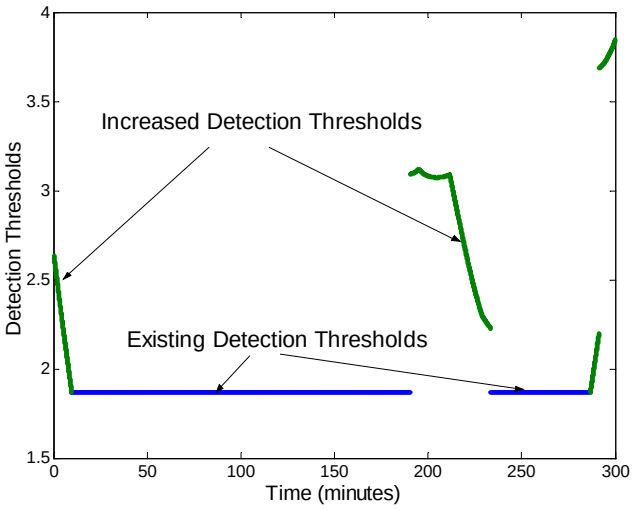

Figure 10: Increase Detection Thresholds Such That Effective VPL_{H0} = VAL

The worst VPL_{HO} obtained from "two-out" SV combinations with the same IMT-PDM dataset are plotted in Fig 9. The number of all possible two-SV-out combinations is $N*(N-1)/2$ permutations, where *N* is the number of measurements or SV's approved by the IMT. The maximum number of measurements is 10 in this dataset, resulting in 45 permutations. Given that *W_VPL*s are less than *VAL*, increased detection thresholds can be applied for sigma monitoring as shown in Fig 10. The existing detection threshold, 1.87, is equal to the inflation

factor with PDM, since out-of-control sigma above the inflation factor is defined as a failure. The increased inflation factor, with which the effective VPL_{HO} would be the same as *VAL*, becomes the new detection threshold. If *W_VPL* is greater than *VAL*, there will be no benefit from using the PDM outputs.

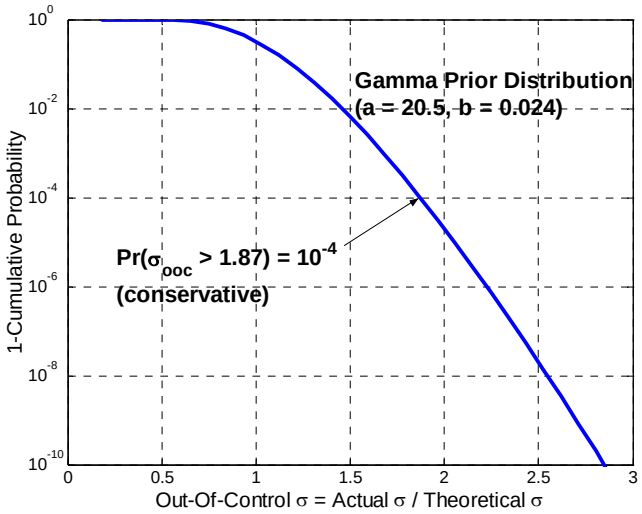

Figure 11: Prior Probability for Out-Of-Control σ

Figure 11 presents a prior probability of out-of-control sigma (σ_{ooc}) modeled as a Gamma distribution with parameters (a=20.5 and b=0.024). The probability for σ_{ooc} to exceed the detection threshold, 1.87, is set to 10^{-4}. Based on this prior probability, probabilities for σ_{ooc} to exceed the new thresholds are computed. The synthetic results demonstrates the improvement on average continuity (*Mean Time Between Failure*) by 27%

7.0 PDM-CUSUM

The PDM plays an important role in providing extra integrity upon the existing sigma monitors, since those cannot detect all cases in which the broadcast σ_{pr_gnd} no longer bounds the true sigma. Regarding this, Cumulative Sum (CUSUM) algorithms were implemented in PDM to detect sigma violations. The same CUSUM method, applied to the range-domain sigma monitoring [4, 16], is used except that the input (Y_n) is the squared and normalized values of vertical position errors (*VPE*). The *VPEs* normalized by their theoretical sigma (σ_{vpe}) projected to position domain are inputs to the CUSUM.

$$Y_n = \left(\frac{VPE - \mu_{vpe}}{\sigma_{vpe}} \right)^2 \qquad \sigma_{vpe} = \sqrt{\sum_{i=1}^{N} S_{vert,i}^2 \sigma_i^2} \tag{6}$$

The details of this algorithm are described in Appendix B.

The Head-Start CUSUM variant has been tested with the IMT-PDM data under nominal conditions. The top plot in Figure 12 displays PDM-CUSUM, and the lower plot shows the normalized *VPE* from (6) that fed the CUSUM. The CUSUM in this case is targeted at an out-of-control sigma 1.87 times that of the theoretical sigma (σ_1 = 1.87), which gives a high windowing factor (k = 1.753). CUSUM is initialized at $h/2$ = 18.9 and is reset there every time the CUSUM falls below zero. Under nominal conditions, the CUSUM slowly falls toward zero, since the normalized VPE^2 is usually below k and k is subtracted off at each epoch. The CUSUM is updated every 200 seconds, which corresponds to two carrier-smoothing time intervals, so that successive updates are statistically independent. The threshold of 37.8 is never threatened, and no flags are observed at all.

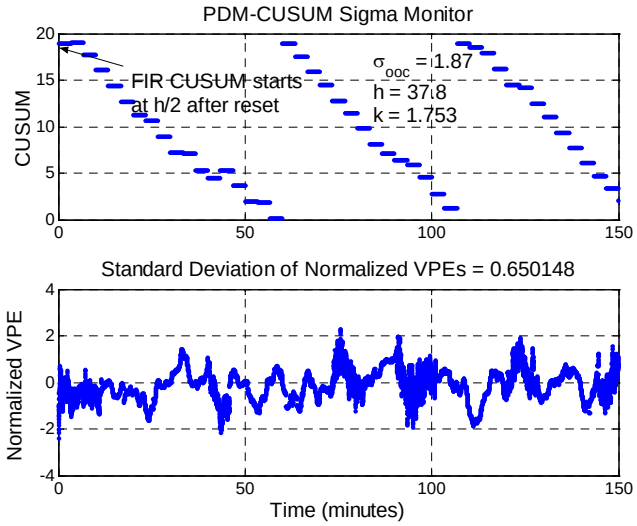

Figure 12: PDM-CUSUM Results from Nominal Data

The range measurement from all reference receivers could possibly be subjected to the same amount of errors in failure conditions. The existing range-domain sigma monitors may not observe such common mode failures (such as multipath correlation), since the those monitors are designed to detect sigma anomalies computed based on the differences between pseudorange corrections across reference receivers. In order to simulate a failure condition like this, controlled errors are injected into IMT-PDM using code-minus-carrier method [4]. Inserting errors into stored nominal receiver packets previously collected by the IMT antennas induces sigma violations. The PR errors on all satellites in view are increased to 3 times the nominal error, and those injected errors are exactly same for all reference receivers.

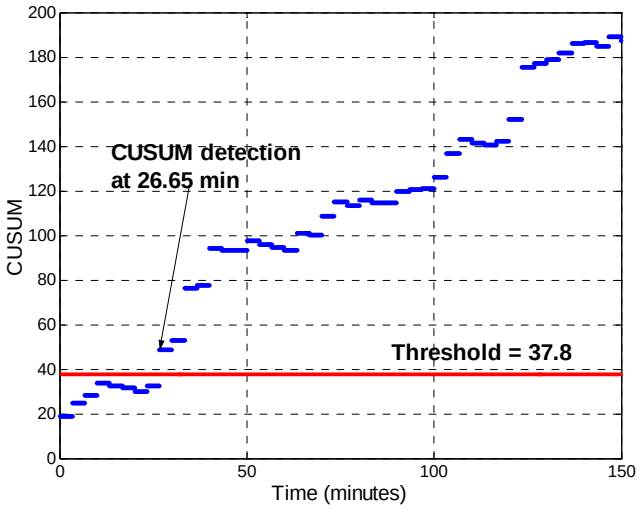

Figure 13: PDM-CUSUM Results from Failure Test
(3 x Error Sigma on All SV; All RR)

Figure 13 shows the result of applying the Head-Start CUSUM variant to failure-injected IMT-PDM. The Head-Start CUSUM, initialized at $h/2$ = 18.9, adds up the increased normalized *VPE* due to severe errors injected on range measurements. The PDM-CUSUM crosses the threshold at 26.65 minutes after fault injection. On the other hand, these anomalies couldn't be detected with the current range-domain sigma monitoring algorithms as expected.

8.0 SUMMARY AND FUTURE WORK

This paper demonstrates the uses of Position Domain Monitor (PDM) by which the existing Category I LGF architecture can be improved to support Category II/III operations. A new methodology to estimate inflation factors of broadcast sigma is presented as a tool to evaluate the user performance. The performance achieved by the PDM appears to be sufficient to meet the stringent availability requirements of Category II/III. In addition, the PDM protection level outputs for subsets of satellites in view are used to lower average continuity loss risk, while maintaining the required integrity. Finally, the CUSUM approach could improve upon the PDM algorithms by providing extra navigation integrity to users.

Combining PDM with the IMT in real time may be necessary in future work to better emulate an operational LGF. This would make it possible for *Executive Monitoring* (EXM) to better isolate faults by getting an access to the processed PDM test statistics (position error, worst *VPL*, and CUSUM). Further improvement of PDM performance is possible with the *Bayesian* CUSUM and is an ongoing work.

ACKNOWLEDGEMENTS

The constructive comments and advice regarding this work provided by many other people in the Stanford GPS research group are greatly appreciated. The authors gratefully acknowledge the Federal Aviation Administration Satellite Navigation LAAS Program Office (AND-710) for supporting this research. The opinions discussed here are those of the authors and do not necessarily represent those of the FAA or other affiliated agencies.

APPENDIX A: DERIVATION OF POSITION SOLUTIONS OF LAAS USER

This appendix provides a derivation of the position solutions for both the PDM and the "pseudo-user".

A.1 Carrier Smoothing

The carrier-smoothing filter is applied with the same method performed in the IMT, to reduce raw pseudorange measurement errors by using the following filter at epoch k [2, 9, 10];

$$PR_s(k) = \frac{1}{N_s} PR(k) + \frac{N_s - 1}{N_s} PR_{proj}(k) \qquad \text{(A-1)}$$

where

$$PR_{proj}(k) = PR_s(k-1) + \phi(k) - \phi(k-1) \qquad \text{(A-2)}$$

$$N_s = \tau_s / T_s \qquad \text{(A-3)}$$

and PR and ϕ are the pseudorange and carrier-phase measurements, respectively. The smoothing filter uses a time constant τ_s of 100 seconds and the sample interval T_s of 0.5 seconds; thus N_s is equal to 200.

A.2 Application of Differential Corrections

The corrected pseudoranges are computed as follows

$$PR_{sc} = PR_s + PRC + RRC * T_s + TC + c * (\Delta t_{sv}) \qquad \text{(A-4)}$$

where *PRC* and *RRC* are the pseudorange correction and the range rate correction from the IMT-approved message. *TC* is the tropospheric correction, *C* is the speed of light, and Δt_{sv} is the satellite clock correction.

A.3 Differential Positioning

Three-dimensional position is computed using a linearized, weighted least squares solution based on the set of differential corrections meeting the requirements of the LAAS MOPS [1]. The basic linearized measurement model is

$$\Delta y = G\Delta x + \varepsilon \qquad \text{(A-5)}$$

where Δx is the four dimensional position/clock vector and Δy is a vector containing the corrected pseudorange measurements minus the expected ranging values based

on the location of the satellites and the location of PDM antenna. G is the observation matrix and ε is a vector containing the errors in y. The weighted least squares estimate of the states can be found by

$$\Delta \hat{x} = S \cdot \Delta y \tag{A-6}$$

where S is the weighted least square projection matrix

$$S \equiv (G^T \cdot W \cdot G)^{-1} \cdot G^T \cdot W \tag{A-7}$$

$$W^{-1} = \begin{bmatrix} \sigma_1^2 & 0 & \cdots & 0 \\ 0 & \sigma_2^2 & \cdots & 0 \\ \vdots & \vdots & \ddots & \vdots \\ 0 & 0 & \cdots & \sigma_N^2 \end{bmatrix} \tag{A-8}$$

and W^{-1} is the inverse of the least squares weighting matrix and σ_i is the fault free error term associated with satellite *i.*

A.4 Pseudorange Error Model

The total differentially corrected pseudorange error is given by:

$$\sigma_i^2 = \sigma_{gnd}^2 + \sigma_{air}^2 \tag{A-9}$$

The ground error is computed as

$$\sigma_{gnd}^2 = \sigma_{pr\_gnd}^2 / M \tag{A-10}$$

where M is the number of reference receivers. The following formula is used to calculate the elevation-dependent σ_{pr_gnd}:

$$\begin{aligned} \sigma_{pr\_\mathrm{gnd}} &= 0.15 + 0.84 e^{-\alpha/15.5}; \quad \alpha \geq 35 \\ &= 0.24; \quad \alpha < 35 \end{aligned} \tag{A-11}$$

where α is the satellite elevation angle in degrees. The Ground Accuracy Designator C (GAD-C) model is applied to the σ_{pr_gnd} model based on the validation in the LAAS MASPS [9]. The airborne errors were substituted by the ground reference receiver error for the purpose of the ground-based PDM and ground-located "pseudo-user".

APPENDIX B: CUSUM MONITOR ALGORITHM

Cumulative Sum (CUSUM) is a superior tool to detect smaller but persistent shifts, and it can be shown to be "optimal" in terms of minimizing time-to-alert under specified failure conditions [17]. The CUSUM starts at zero or a head-start value of $H^+ > 0$ and then increments each epoch by the size of the monitored input Y minus the desired 'failure slope' k that is based on a target out of control sigma (σ_1) that represents 'failed' performance.

$$\begin{aligned} C_0^+ &= 0 \quad (\text{or use 'head start': } H^+) \\ C_n^+ &= \max\left(0,\ C_{n-1}^+ + Y_n - k\right) \end{aligned} \tag{B-1}$$

$$k_{\mathrm{sigma}}^+ = -\frac{\ln(\sigma_0) - \ln(\sigma_1)}{\left(2\sigma_1^2\right)^{-1} - \left(2\sigma_0^2\right)^{-1}}^2 \tag{B-2}$$

If the CUSUM falls below the initial value (zero or head-start value) on a given epoch, it is reset to zero. If the sum is above zero at any update epoch, the CUSUM is compared to a fixed threshold (h) that does not vary with time. The threshold is determined based on the desired average run length (ARL) and k [17]. If it accumulates to above the threshold, an alert is issued.

REFERENCES

1. *Minimum Operational Performance Standards for GPS/Local Area Augmentation System Airborne Equipment*. RTCA DO-253A, SC-159, WG-4A. Nov. 28, 2001, Washington, D.C.
2. *Specification: Performance Type One Local Area Augmentation System Ground Facility*. FAA-E-2937. 21 September 1999, Washington, D.C.: U.S. Federal Aviation Administration.
3. *Specification: Category I Local Area Augmentation System Non-Federal Ground Facility.* FAA/AND710-2937. May 31, 2001, Washington, D.C.: U.S. Federal Aviation Administration.
4. Lee, J., et al. *LAAS Sigma Monitor Analysis and Failure-Test Verification*. in *ION NTM 2001*. June 11-13, 2001. Albuquerque, N.M.
5. Braff, R., *Position Domain Monitor (PDM) Performance Analysis for CAT III*. 2002, MITRE/CAASD: McLean, VA.
6. Lee, J., et al. *LAAS Position Domain Monitor Analysis and Failure-Test Verification*. in *21st AIAA ICSSC*. April, 2003. Yokohama, Japan.
7. Luo, M. and S. Pullen, *LAAS Reference Receiver Correlation Analysis*. Unpublished Manuscript. Feb. 17, 1999: Stanford University.
8. Xie, G., et al. *Integrity Design and Updated Test Results for the Stanford LAAS Integrity Monitor Testbed*. in *ION NTM*. June 11-13, 2001. Albuquerque, N.M.
9. *Minimum Aviation System Performance Standards for the Local Area Augmentation System (LAAS).* RTCA/DO-245, SC-159, WG-4. September 1998, Washington D.C.
10. *FAA LAAS Ground Facility (LGF) Functions.* Unpublished Manuscript. Vol. 2.4. September 9, 1998: LAAS KTA Group.

11. Pervan, B. and I. Sayim, *Sigma Inflation for the Local Area Augmentation of GPS.* IEEE Transactions on Aerospace and Electronic Systems, October, 2001. **Vol. 37**(No. 4).

12. Pervan, B., S. Pullen, and I. Sayim. *Sigma Estimation, Inflation, and Monitoring in the LAAS Ground System*. in *Proceedings of ION GPS*. Sept. 19-22, 2000. Salt Lake City, UT.

13. DeCleene, B., *Proof for ICAO Overbounding Requirement.* December 1999, ICAO Overbounding Subgroup.

14. Gary, M., et al. *Development of the LAAS Accuracy Models.* in *Proceedings of ION GPS*. Sept. 19-22, 2000. Salt Lake City, UT.

15. Pullen, S., et al. *LAAS Ground Facility Design Improvements to Meet Proposed Requirements for Category II/III Operations*. in *Proceedings of ION GPS*. Sept, 2002. Portland, OR.

16. Pullen, S., et al. *The Use of CUSUMs to Validate Protection Level Overbounds for Ground Based and Space Based Augmentations Systems*. in *Proceedings of ISPA 2000*. 18-20 July 2000. Munich, Germany.

17. Hawkins, D.M. and D.H. Olwell, *Cumulative Sum Charts and Charting for Quality Improvement.* 1998, Springer-Verlag, Inc.: New York.